RESEARCH PAPER

Design and performance validation of a novel 3d printed thin-walled and transparent electron beam applicators for intraoperative radiation therapy with beam energy up to 12 MeV

Agnieszka Misiarz[1], Aleksandra Lenartowicz[1], Przemysław Adrich[1], Jacek Rzadkiewicz[1], Sławomir Wronka[1], Jan Trzuskowski[1], Marta Kruszyna-Mochalska[2, 3], Bartosz Urbański[3, 4], Beata Adamczyk[5], Jacek Pracz[6]

[1]National Centre for Nuclear Research, Otwock–Swierk, Poland
[2]Department of Medical Physics, Greater Poland Cancer Centre, Poznan, Poland
[3]Department of Electroradiology, Poznan University of Medical Sciences, Poznan, Poland
[4]Department of Brachytherapy, Greater Poland Cancer Centre, Poznan, Poland
[5]Department of Breast Surgical Oncology, Greater Poland Cancer Centre, Poznan, Poland
[6]Centre of High Technologies "HITEC ŚWIERK" Ltd, Otwock, Poland

ABSTRACT

A high-energy electron accelerator is used in the treatment of patients in the so-called intraoperative electron radiotherapy (IOERT). The work aimed to present the results of the validation of a new design of an electron beam applicator for use in IOERT. A novel solution was described along with the design optimization method based on Monte Carlo simulations. In this solution, the applicator consists of two parts. The lower exchangeable part collimates the therapeutic field. Measurements were made based on the International Electrotechnical Commission (IEC) standard recommendations. The measurement described in the standard has been adapted to the specificity of the intraoperative accelerator Source to Skin Distance — of 60 cm and applicators with a circular cross-sectional area. Measurements were performed for nominal beam energies of 6, 10, and 12 MeV and two therapeutic field diameters of 6 and 10 cm. The dose due to stray X-ray radiation in all energies is less than 0.3% and increases for energies from 6 to 12 MeV by 2.9 times from 0.1 for 6MeV to 0.29 for 12 MeV. The average dose due to leakage radiation also shows an increasing trend and is higher for a 6 cm diameter applicator. Validation confirmed the usefulness of the novel applicator design for clinical applications. Thanks to the use of 3D printing, it was possible to make applicators that are transparent, biocompatible and, at the same time, light and form a beam field with therapeutically useful accuracy, and the leakage radiation does not exceed normative recommendations.

Key words: IOERT; electron linear accelerator; electron applicator

Rep Pract Oncol Radiother 2024;29(3):329–339

Introduction

The high-energy (MeV) electron accelerators, apart from low-kV X-ray systems, are intended for use in the treatment of patients in the so-called intraoperative radiotherapy (IORT) [1, 2].

Compared to conventional external beam radiotherapy (EBRT), intraoperative electron radiother-

Address for correspondence: Agnieszka Misiarz, Department of Nuclear Techniques and Equipment, National Centre for Nuclear Research, Otwock, Poland; e-mail: agnieszka.misiarz@ncbj.gov.pl

apy (IOERT) irradiation is performed during a surgical procedure. In intraoperative therapy, the dose is delivered only in one fraction during tumor resection surgery. This leads to a reduction in the total time of radiotherapy application. IOERT is targeted, i.e. restricted to the irradiation area prepared by the surgeon during the operation. The radiation therapy team (doctor and medical physicist) select the parameters of the electron beam to deliver the planned therapeutic dose directly to the target area. The constant distance between the radiation source, the end of the applicator, and the surface of the irradiated tissue enables quick and simple calculation of the number of monitor units needed for the prescribed dose. The targeted nature of IOERT, which allows for minimizing the geographical error and significantly reducing the dose in healthy tissues, makes this method suitable for repeated radiotherapy — where dose distributions obtained by conventional methods are unsatisfactory and, consequently, conventional radiotherapy is not recommended [3].

One of the crucial elements of the IOERT accelerator is the applicator whose primary task is to deliver the electron beam to the tumor bed precisely, minimize exposure to normal tissues, and suppress the side radiation. The applicator consists of two parts: the upper one located at the end of the accelerator head and the lower one intended for use in direct contact with the patient during irradiation. Since it is used in the operating room and its lower part is inserted into the postoperative wound, it must be made of a material that is easy to sterilize.

There are two ways to mount applicators for intraoperative accelerators on the accelerator head - hard and soft docking. In the first one, the two parts of the applicator are connected using a connecting element, the other method is non-contact, consisting in bringing the applicator closer to the accelerator head at an appropriate distance so that the axis of the radiation beam is aligned with the long axis of the applicator.

Currently, two companies in the world are manufacturers of accelerators dedicated to IOERT. In both cases, the electron beam applicators have a circular shape with an internal diameter (forming the size of the irradiation field) of a maximum of 10 cm. The materials used for the applicators are anodized aluminum or stainless steel, and polymethyl methacrylate (PMMA). The length of the lower part of the applicator is 30 cm for the first and 23 or 31 cm for the other available device. Due to its weight and the method of docking (soft docking), special attachments to the operating table are provided for applicators made of aluminum or steel, which, also due to the mechanical structure of the entire accelerator, must be specially dedicated for a given operating room in which irradiation is performed [10, 11].

The work presented here is aimed at assessing the possibility of making thin-walled and transparent applicators for intraoperative radiotherapy that would simultaneously meet the normative requirements concerning the radiation safety of the patient and medical personnel.

Materials and methods

Description of the electron linear accelerator system and applicators

The AQURE accelerator is a radiotherapeutic device designed and manufactured at the National Center for Nuclear Research (NCBJ, Poland) that produces electron beams with energies ranging from 4 to 12 MeV [13]. For standard intraoperative radiotherapy, the maximum dose rate is 10 Gy/min. The accelerator is built on a movable base ensuring the movement of the whole and ensuring the possibility of moving the head relative to the base. The therapeutic head can be tilted in two planes and can be rotated on the column (Fig. 1). Thus, from a mechanical point of view, the intraoperative accelerator is both an electron accelerator and a mobile manipulator, allowing the head to be set in a specific position within a relatively large working space.

Due to the targeted nature of the therapy, the radiotherapist must be able to place the applicator over the target as accurately as possible. To properly collimate the beam of electron radiation, applicators limiting/adjusting the radiation field to the field of the target volume should be used [1, 2]. The applicators are designed not only to form the therapeutic beam but also to limit the dose outside the collimated irradiation field (according to the PN EN 60601-2-1 standard) [4]. Accessories used to limit the radiation field and modify the dose (applicators, tissue-like boluses, shield plates) and all elements that have direct contact with the operating field should be made of materi-
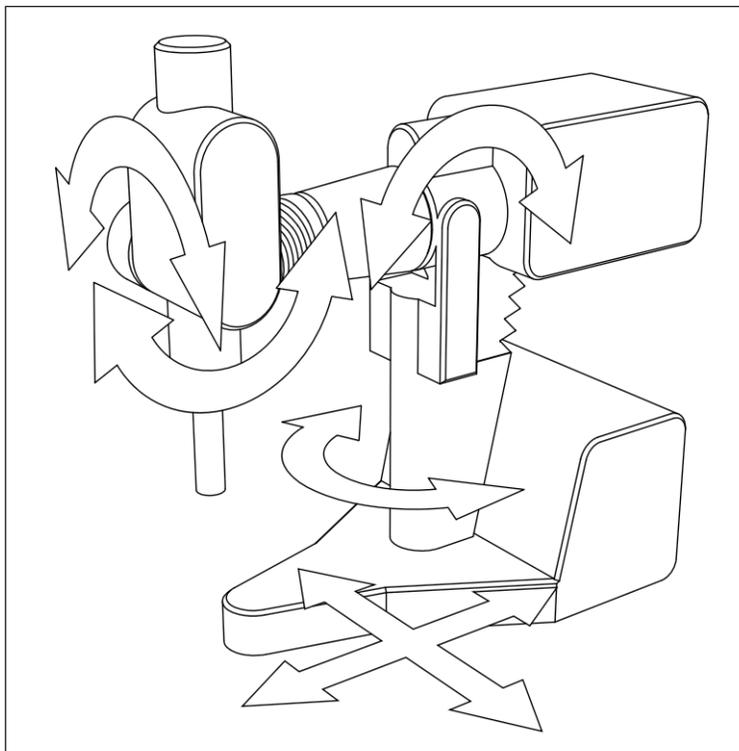
Figure 1. Intraoperative accelerator AQURE movements

als that allow sterilization, without changing their physical properties [5].

To meet both of the above requirements, the lower part of electron applicators used in the intraoperative accelerator AQURE are made of a transparent biocompatible material MED610. MED610 is a material used in 3D printing using PolyJet technology. This is a type of resin that, in a print with a resolution of 0.019 mm, achieves a density similar to PMMA (according to producer declaration) [15]. The material is intended for both medical and dental applications and is certified for permanent use on skin contact (over 30 days) and limited contact with mucous membranes (up to 24 hours). The applicator is attached using the hard-docking method, after placing the applicator in the patient's body. Using the control cassette, the operator directs the movement of the accelerator and the head, so that after reaching the operating table it is possible to connect the upper part of the applicator (located at the end of the accelerator head) with the lower one (placed in the patient).

The lower part of the applicator is made of MED610 resin, which ensures its transparency, easy sterilization, and correct placement of the applicator part in the tumor bed; is designed for hard

docking, and its maintenance in the right position, until it is fastened to the part on the head, does not require the use of additional, dedicated fastening (Fig. 2). Thanks to the use of a new solution for the shape of the walls, as described further below, the applicator effectively limits the leakage radiation in compliance with the IEC standard [4] and without the need for unpractically thick walls. A detailed description of the applicator design is the subject of the patent [6].

Applicator design optimization

The optimal design of the beam forming and collimation system, and in particular of the shape of the transparent part of the beam applicators, was achieved as a result of an iterative improvement procedure based entirely on Monte Carlo simulations, as described further below and in more detail in our previous works [7–9].

As depicted in Figure 2, the beamforming and collimation system consists of primary and secondary scattering foils, a primary collimator, and an applicator. There are also two independent ionization chambers in the way of the electron beam located next to the secondary scattering foil and in front of the primary collimator.
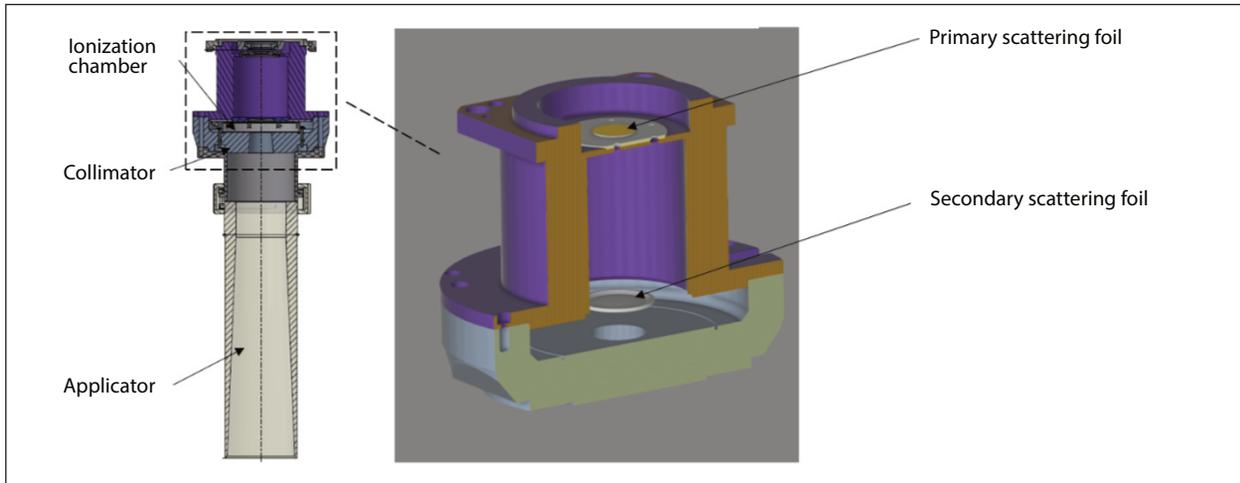
Figure 2. Scheme of an applicator with a diameter of 100 mm designed to be made of a biocompatible transparent material (MED610) for AQURE IOERT accelerator. Enlarged view of the layout of scattering foils in the collimator

The design optimization starts with the preliminary design of the primary and secondary scattering foils. The foils are first designed in a simplified model of the system geometry (Fig. 3), in particular with the applicator modeled as a simple tube of constant thickness over the entire length. This initial design of the foils is necessary to op-timize the construction of the applicators. Once the final design of the applicators is completed, the secondary foil is fine-tuned to eliminate any possible deterioration of dose homogeneity over the therapeutic field, which could arise from the modifications introduced to the geometry of the applicator.

For the design and optimization of the scattering foils, we adopted the methodology developed in our previous works [7–9]. As is well known [7; and references therein], a combination of flat primary scattering foil and a secondary scattering foil of thickness profile described by a Gaussian function:

$$h(r) = H \, exp(-r^2/R^2)$$

could produce a uniform off-axis beam profile. While for a given beam energy and geometry of the beamforming system, it is reasonably straightforward to find optimal thickness of the primary scattering foil, it is much more involved to find optimal secondary scattering foil. To this end, one has to minimize the flatness function $f(H, R)$ that describes the variation of the flatness of the off-axis dose profile with respect to parameters H and R of the secondary scattering foil. In a complex geometry of the beamforming system, the function $f(H, R)$ can only be computed using a detailed Monte Carlo simulation, as shown in [8].

This methodology was originally developed to design optimal scattering foils for a system op-

Figure 3. Simplified model of the beam forming system used for preliminary design of the primary and secondary scattering foils

erating with a beam of single energy and with a fixed size of the irradiation field. Here, we extended the methodology to simultaneously consider beams of several energies in the range of 6–12 MeV and fields with different diameters in the range of 5–10 cm. This enabled designing a system equipped with a single primary scattering foil and a single secondary scattering foil that for all combinations of beam energy and therapeutic field diameter delivers beams with the highest possible therapeutic depth and the best possible flatness of the dose profile, while simultaneously causing the least contamination with undesired stray X-ray radiation.

Once the preliminary design of the scattering foils was complete, the geometry of applicators could be optimized. The main goal was to minimize the thickness (and thus weight) of the lower, transparent part of the applicator while simultaneously keeping the leakage radiation outside the therapeutic field below limits recommended by the appropriate standards and guidelines [4, 5], even for the beam of the highest considered nominal energy of 12 MeV. From the clinical point of view, the wall of the applicator should be as thin as possible to achieve the best cosmetic results of the surgical intervention, especially in the case of breast cancer treatment.

The geometry of the lower, transparent part of the applicator is depicted in Figure 4. Contrary to other solutions, here, the thickness of the applicator wall gradually decreases towards its bottom end.

In an iterative adjustment procedure, parameters describing the variation of the applicator wall thickness were optimized. The objective was to achieve the thinnest possible wall at the bottom of the applicator, i.e., at this end that is inserted into the surgical field, while keeping the leakage radiation below the level recommended by the IEC standard [4].

In the final step of the design optimization, the shape of the secondary scattering foil was fine-tuned by recomputing the function $f(H, R)$ and finding its minimum for the final geometry of the system. This was to improve the uniformity of the off-axis beam profile that deteriorated somewhat as a result of changes in beam interaction with the modified inner wall of the lower part of the applicator. As a result, in the final design, flatness of the calculated off-axis beam profile is below 3% for
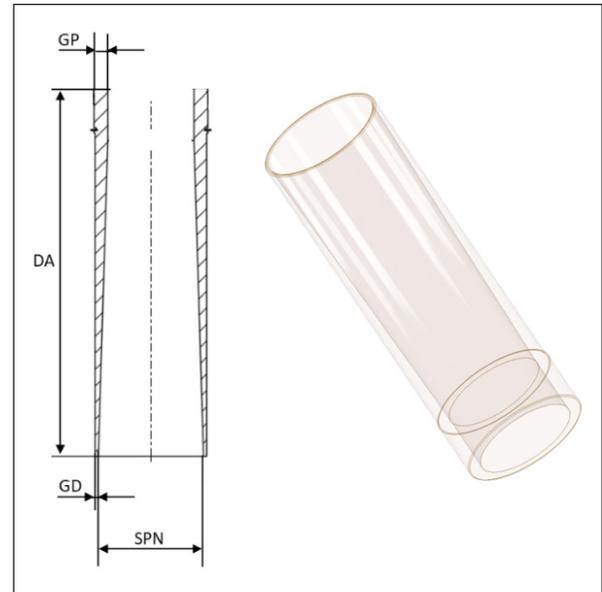

Figure 4. Lower part of the applicator. GP — upper thickness of the applicator walls; GD — lower thickness of the applicator walls; DA — total length of the lower part of the applicator; SPN — size of the radiation field determined by the applicator

all combinations of beam energy and applicator diameter.

Geant4 application was used to perform Monte Carlo simulations as described in detail in our previous work [9]. Certain simplifications regarding the source beam as well as system geometry were applied in the simulations performed throughout the design optimization. The primary electron beam was simulated as monoenergetic with momentum direction parallel to the z-axis while in the plane perpendicular to the z-axis the beam had Gaussian position distribution in both axes with FWHM = 3 mm. The geometry of the Monte Carlo model was axially symmetric and was constructed of simple geometrical solids. The inner surfaces of all the elements with which the beam could directly interact were modeled realistically while the outer surfaces were simplified and did not account for all the details of the final engineering model. In particular, all the mechanical structures that could not influence the beam propagation were not taken into account. Furthermore, materials were also modeled with several simplifications. While in the fabricated device there are many parts made of different aluminum alloys, e.g., secondary scattering foil, scattering foils' supports, primary collimator, upper part of the appli-

cator, etc., for the Monte Carlo simulation, they were modeled as composed of pure aluminum. The lower part of the applicator is 3d printed and made of biocompatible transparent material under the tradename "MED610". According to the manufacturer's specification, this material includes a significant fraction of proprietary ingredients of undisclosed chemical composition. In the simulation, the lower part of the applicator was modeled as composed of PMMA of density corresponding to a nominal density of MED610.

The simulated dose due to leakage radiation was registered in strict analogy to the guidelines for the measurements (see next Section), i.e., at 1 cm depth in water, in a series of concentric rings of 1 cm width as schematically depicted in Figure 6.

The off-axis dose profile was registered in water at a depth of 9 mm for the 6 MeV beam and at 19 mm for the beams of higher energy. The off-axis dose was registered in a model of a detector consisting of concentric rings of 2 mm thickness and radius increasing in steps of 2.5 mm as described in detail in [9].

Methodology for measuring the parameters of IOERT beam shaped with the MED610 applicator

Measurements were made based on the IEC 60601-2-1 standard regarding leakage radiation and the IEC 60976 regarding the beam profile [4]. The measurements described in the standard have been adapted to the specificity of the intraoperative accelerator - SSD (Source to Skin Distance) 60 cm and applicators with a circular cross-sectional area. The measurements were made using a Markus ionization chamber PTW Freiburg (type 34045) in the MP3 PTW water phantom. The measurement results were collected using MEPHYSTO mc2 PTW software [12].

The M field is determined by the angle of the beam collimator at the SSD (Source to Skin Distance). On the other hand, M10 is formed from the field M where its diameter has been increased by 10 cm. Because of the collimator used in the AQURE accelerator (10.5 degrees), the size of the M field in SSD 60 cm is only 110.3 mm, the M10 field was used to calculate the average dose from leakage radiation. The dimensions of the M and M10 are shown in Figure 5.

According to the IEC 60601-2 standard, electron beam applicators shall be provided. Each electron beam applicator shall attenuate all ionizing radiation (excluding neutron radiation that is not expected for the considered electron beams) incident on electron beam applicators and other parts of the radiation head, and limit leakage radiation outside the electron radiation field, in the area M10 which includes M and any area outside M that results from extending the periphery of the geometrical radiation field by 10 cm [4].

The average absorbed dose at a distance of 4 cm from the inner wall of the applicator to the border of the M10 area should not exceed 1% of the maximum dose in the beam axis. The geometry of this measurement is shown in Figure 6.

The task of the applicator, apart from limiting leakage radiation, is to properly form the electron beam into a field determined by its diameter. The basic measurement checking the distribution of the radiation field is
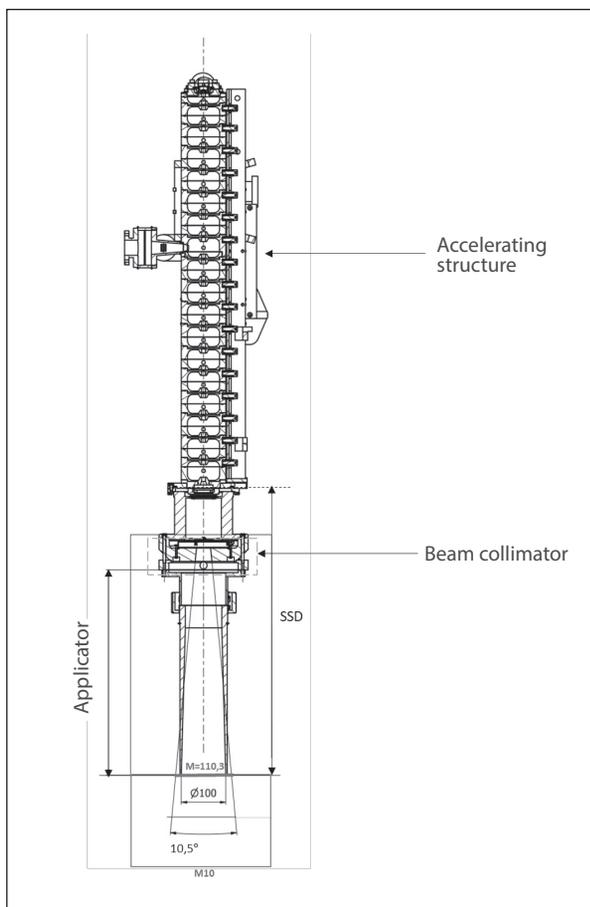

Figure 5. The beam limiting system geometry for the AQURE accelerator with M and M10 area
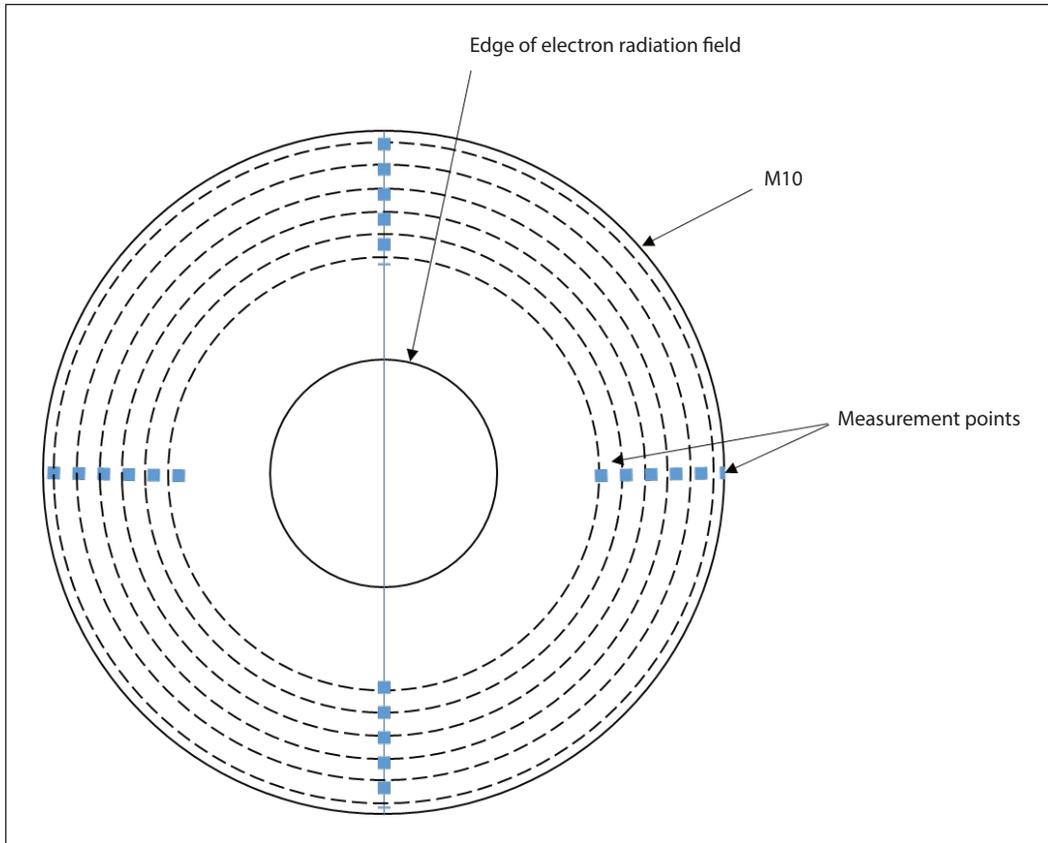
Figure 6. The geometry of the average absorbed dose outside the M10 area measurement

the off-axis profiles measurement. To compare the convergence of the off-axis profiles with the simulations, measurements were also made at the same depths in the water as the simulations. It was 9 mm for energies up to 6MeV and 19 mm for higher energies. Diode detectors PTW (microSilicon type 60023) and water phantom MP3 were used to create these radiation dose profiles. The measurement results were collected using MEPHYSTO mc2 PTW software.

The field profiles were compared point by point and the dose difference and standard deviation from the mean of the differences between simulations and measurement were calculated.

Results

Simulations performed with monoenergetic beams predicted good homogeneity of the delivered dose for all combinations of beam energies and field sizes as presented in Table 1. Simultaneously, the calculated dose in the patient plane outside the field due to the leakage radiation is below regulatory requirements, i.e. below 1% of the dose maximum for the beam energy equal to or less than 10 MeV and below 1.2% for the 12 MeV beam.

Table 1 shows Monte Carlo calculated flatness of the off-axis dose profile for monoenergetic beams of 6, 10, and 12 MeV energy, and for applicators of

Table 1. Monte Carlo calculated flatness of the off-axis dose profile for monoenergetic beams of 6, 10, and 12 MeV energy, and for applicators of diameters ranging from 5 to 10 cm with 1 cm steps

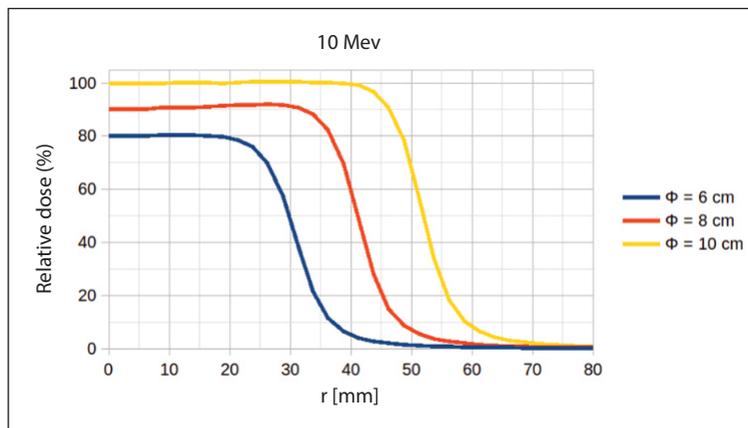| Beam energy [MeV]	Field diameter [cm]					
	5	6	7	8	9	10
6	2.7	1.4	0.9	1.7	2.0	1.6
10	2.7	1.7	1.4	2.2	2.4	1.0
12	0.6	1.9	2.7	2.3	1.0	3.0

Figure 7. Monte Carlo simulations of electron beam off-axis profiles

Table 2. Selected therapeutic beam parameters resulting from Monte Carlo simulations with primary beam energy spectra calculated using General Particle Tracer (GPT) code (upper part of the Table) compared to measurements (lower part of the Table)

Energy [MeV]	6 MeV		10 MeV		12 MeV	
Results of simulations						
Applicator diameter [cm]	6	10	6	10	6	10
Flatness of the off-axis profile (%)	1.98	1.16	0.96	1.43	1.28	2.85
Dose due to stray X-ray radiation (%)	0.10	0.10	0.16	0.12	0.29	0.15
Average dose in M_{10} area due to leakage radiation (%)	0.28	0.22	0.97	0.65	1.07	0.95
Results of measurements						
Applicator diameter [cm]	6	10	6	10	6	10
Flatness of the off-axis profile (%)	1.8	2.4	1.7	2.8	1.4	2.7
Dose due to stray X-ray radiation (%)	0.07	0.10	0.15	0.17	0.18	0.25
Average dose in M_{10} area due to leakage radiation (%)	0.22	0.19	0.83	0.72	1.5	1.23

diameters ranging from 5 to 10 cm with 1 cm steps. The off-axis profiles were calculated at a depth of 9 mm in water for the 6 MeV beam and at a depth of 19 mm for the beams of higher nominal energies.

Figure 7 shows an example of Monte Carlo calculated off-axis dose beam profiles. The presented profiles were calculated in water for a 10 MeV electron beam at three different diameters of the field 6, 8, and 10 cm.

Once the design was completed and the entire system manufactured, the Monte Carlo simulations were performed in the final geometry with more realistic primary beam energy spectra as calculated using the General Particle Tracer (GPT) code [14]. Selected parameters of the therapeutic beams resulting from these simulations for nominal beam energies of 6, 9, and 12 MeV and two different therapeutic field diameters of 6 and 10 cm are pre-sented in Table 2. Here, the dose due to stray X-ray radiation was determined on the beam axis, 10 cm below the depth of 10% isodose.

Measurement results, parameters of the therapeutic beams for nominal beam energies of 6, 10, and 12 MeV and two different therapeutic field diameters of 6 and 10 cm are presented in Table 2.

For a given energy, the flatness of the off-axis profile was calculated as a percentage difference between the maximum and minimum dose in the flattened region. That region is defined as field size at 90% isodose minus 1 cm. The dose due to stray X-ray radiation for beams of all energies is less than 0.3% and increases for energies from 6 to 12 MeV by 2.9 times from 0.1% for 6MeV to 0.29% for 12MeV. The average dose in the M10 area due to leakage radiation also shows an increasing trend and is higher for a 6 cm diameter applicator.
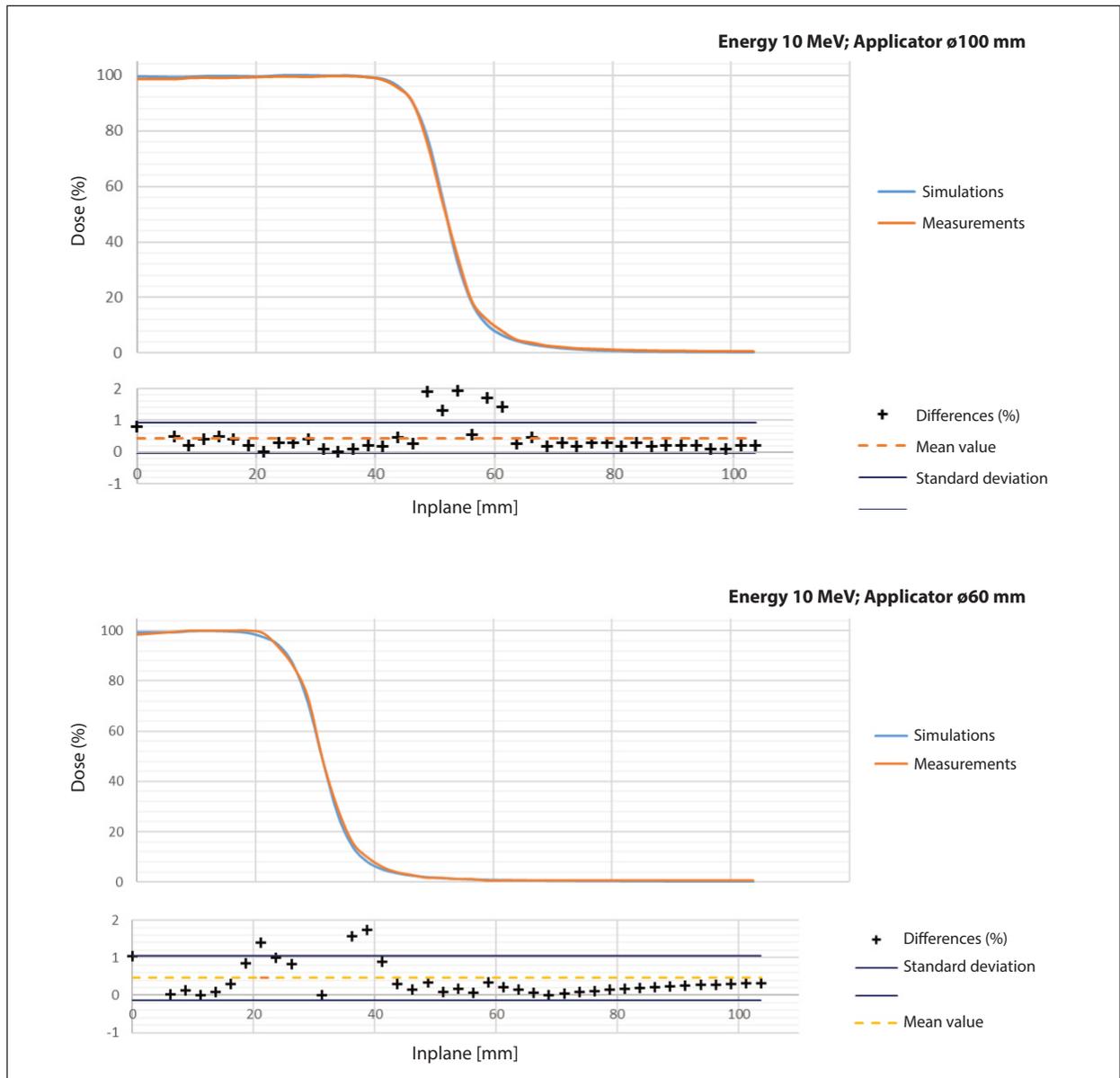
Figure 8. Inplane profile comparison for 10 and 6 cm circular field applicator; blue — simulations, orange — measurements

Figure 8 shows a comparison of the off-axis profiles for two applicator sizes: 6 and 10 cm. The percentage difference between the measured value and the simulated value was calculated for each measurement point and simulation. The standard deviation from the average percentage difference between the measurement points and the simulation is also marked on the chart.

Discussion

Performed optimization resulted in the design in which the wall at the bottom of the lower part of the applicator is only 3 mm thick for all considered field sizes. The design of the applicator is independent of the beam energy. In addition, applicators for all field diameters are of the same length. The wall thickness at the top of the lower part of the applicator depends on the field diameter and is larger for the wider fields.

Due to simplifications of the models used in the Monte Carlo, the results of the simulations and the measurements differ in details, however, they quite well agree concerning the general trends. The flatness of dose profiles, simulated and measured, is below 3% for each beam energy and field

size combination. The dose due to stray X-ray radiation grows with beam energy and is below 0.3% even for the beam of the highest energy. This is expected behavior as the majority of the X-ray radiation originates as Bremsstrahlung in the scattering foils and cross-section for Bremsstrahlung emission increases with electron energy.

There is a large deviation in Monte Carlo calculations concerning the average dose due to leakage radiation for the beam of the highest energy. While calculations performed with a 12 MeV monoenergetic primary beam result in a dose due to leakage radiation below 1.2%, the same calculations performed with an energy spectrum simulated with the GPT code predicted doses due to leakage radiation up to 1.5%. Interestingly, the measured dose due to leakage radiation for the nominal 12 MeV beam is at most 1.07%. The observed differences could be attributed in part to the uncertainty of the composition of the MED610 material used to 3d print the lower part of the applicator and in part to a discrepancy between the GPT-calculated beam energy spectrum and the energy spectrum of the nominal 12 MeV beam of the AQURE accelerator.

An interesting feature revealed from the measurements is the dependence of the stray X-ray radiation dose on the diameter of the applicator. For the beams of 10 and 12MeV nominal energy, the dose due to stray X-ray radiation is higher for the 6 cm applicator than for the 10 cm. This effect is not observed in the Monte Carlo simulations. Although the origin of this behavior and the discrepancy with the trend observed in the simulations is yet to be explained, it bears no important practical consequences.

Figure 8 shows that the differences between the simulated and measured off-axis dose profiles for both irradiation field sizes are within one standard deviation from the mean for more than 90% of the measurement points. This confirms that the model adopted for simulation has been correctly verified in real measurements on the device. Thanks to the shape of the applicator walls, the field it forms, despite the use of light material, meets the normative recommendations for this element of the device.

Conclusion

A novel solution of the electron beam applicator for IOERT was described in this work along with the method of the design optimization based on Monte Carlo simulations.

In this solution, the applicator consists of two parts. The upper part has dimensions independent of the therapeutic field and is attached to the accelerator. The lower exchangeable part collimates the therapeutic beam to the diameter of the desired therapeutic field. During the irradiation procedure, its bottom end is going to be inserted into the surgical bed in the patient while from the top it is going to be hard docked to the upper part of the applicator.

The lower part of the applicator has several advantages compared to previous solutions. It is made of a biocompatible transparent material with a density similar to PMMA, which ensures its transparency, ease of sterilization, and correct placement of the applicator part in the operative bed.

Performed optimization resulted in the design in which the wall at the bottom of the lower part of the applicator is only 3 mm thick for all considered field sizes. This is advantageous from the surgical point of view.

It is made of light material and designed for permanent docking (hard docking), and maintaining it in the appropriate position until it is connected to the part on the head does not require the use of additional, dedicated mounting.

Thanks to the use of a new wall shape solution, the applicator also limits the leakage radiation below the limits recommended by the IEC standard, without the need to use thick external walls.

Results of the measurements show that the proposed shape of the applicator meets both the normative recommendations for forming the radiation field in the beam, as well as the protection against leakage radiation outside the applicator.

Conflict of interests
Author declare no conflicts of interests.

Funding

References

1. Pilar A, Gupta M, Ghosh Laskar S, et al. Intraoperative radiotherapy: review of techniques and results. Ecancermedicalscience. 2017; 11: 750, doi: 10.3332/ecancer.2017.750, indexed in Pubmed: 28717396.

2. Hensley FW. Present state and issues in IORT Physics. Radiat Oncol. 2017; 12(1): 37, doi: 10.1186/s13014-016-0754-z, indexed in Pubmed: 28193241.

3. Rosi A, Viti V. Istituto Superiori di Sanità. Guidelines for quality assurance in intra-operative radiation therapy. Oncología (Barcelona). 2004; 27(7), doi: 10.4321/s0378-48352004000700013.

4. PN-EN IEC 60601-2-1:2021-12 - Medical electrical equipment - Part 2-1: Particular requirements for the basic safety and essential performance of electron accelerators in the range 1 MeV to 50 MeV.

5. Kruszyna-Mochalska M, Bijok M, Pawałowski B, et al. w wsp. Zalecenia Polskiego Towarzystwa Fizyki Medycznej dotyczące kontroli jakości w radioterapii śródoperacyjnej promieniowaniem elektronowym (IOERT) za pomocą mobilnych akceleratorów. Inż i Fiz Med. 2019; 8(1): 7–25.

6. Aplikator terapeutycznej dawki promieniowania jonizującego. Biletyn Urzędu Patentowego. Wynalazki i wzory użytkowe. 2022; 32(P.436884).

7. Adrich P. A new method for designing dual foil electron beam forming systems. II. Feasibility of practical implementation of the method. Nuclear Instruments and Methods in Physics Research Section A. 2016; 817: 100–108, doi: 10.1016/j.nima.2016.02.006.

8. Adrich P. A new method for designing dual foil electron beam forming systems. II. Feasibility of practical implementation of the method. Nucl Instrum Methods Phys Res A. 2016; 817: 100–108.

9. Adrich P. Technical Note: Monte Carlo study on the reduction in x-ray contamination of therapeutic electron beams for Intraoperative Radiation Therapy by means of improvements in the design of scattering foils. Med Phys. 2019; 46(8): 3378–3384, doi: 10.1002/mp.13647, indexed in Pubmed: 31173366.

10. LIAC HWL: the best way to perform IOeRT. https://www.soiort.com/liac-hwl/.

11. Mobetron IORT. https://intraop.com/mobetron-iort/.

12. Advanced Markus® Electron Chamber. https://www.ptwdosimetry.com/en/products/advanced-markus-electron-chamber.

13. Dróżdż A, Waluś M, Zieliński M, et al. Verification of electron beam parameters in an intraoperative linear accelerator using dosimetric and radiobiological response methods. Rep Pract Oncol Radiother. 2021; 26(6): 1029–1034, doi: 10.5603/RPOR.a2021.0128, indexed in Pubmed: 34992877.

14. van der Geer B, de Loos M. The general particle tracer code: design, implementation and application. Ph.D. Thesis, Technische Universiteit Eindhoven, Eindhoven 2001.

15. Biocompatible Clear MED610. https://cadxpert.pl/wp-content/uploads/2019/03/spec_PolyJet_MED610_MED620.pdf.